Cone Breakthrough Time for Horizontal Wells

Paul Papatzacos, Rogaland U.; **T.R. Herring,** SPE, Fina Exploration Norway; **Rune Martinsen,** SPE, Enterprise Oil Norge Ltd.; and **S.M. Skjaeveland,** SPE, Rogaland U.

Summary. Recovery from an oil zone underlying a gas cap, overlying an aquifer, or sandwiched between gas and water can be improved by repressing the coning problem through horizontal-well drainage. Literature methods to predict coning behavior are limited to steady-state flow conditions and determination of the critical rate. The results in this paper are based on new semianalytical solutions for time development of a gas or water cone and of simultaneous gas and water cones in an anisotropic infinite reservoir with a horizontal well placed in the oil column. The solutions are derived by a moving-boundary method with gravity equilibrium assumed in the cones. For the gas-cone case, the semianalytical results are presented as a single dimensionless curve (time to breakthrough vs. rate) and as a simple analytical expression for dimensionless rates $> \frac{1}{3}$. For the simultaneous gas- and water-cone case, the results are given in two dimensionless sets of curves: one for the optimum vertical well placement and one for the corresponding time to breakthrough, both as functions of rate with the density contrast as a parameter. The validity of the results has been extensively tested by a general numerical simulation model. Sample calculations with reservoir data from the Troll field and comparison with test data from the Helder field demonstrate how the theory can be used to estimate the time to cone breakthrough and its sensitivity to the uncertainties in reservoir parameters.

Introduction

Ekrann[1] showed that the critical rate for coning toward a horizontal or vertical well approaches zero as the distance to the outer open boundary approaches infinity. The practical use of critical rates computed from steady-state flow situations is therefore questionable. Ekrann suggested that the time to cone breakthrough is a more relevant parameter.

In a review of the reservoir engineering methods for predicting horizontal-well behavior, Joshi[2] briefly discussed gas and water coning characteristics and stated that no information is available for calculation of breakthrough time for water and gas cones. Giger[3] and Karcher *et al.*[4] present formulas to calculate critical rates for coning toward horizontal wells during steady-state flow conditions. Chaperon[5] solved the same problems with the Muskat[6] method by neglecting the cone-shape influence on the flow pattern.

To the best of our knowledge, Refs. 7 through 9 describe the only methods available for analytic prediction of cone evolution toward horizontal wells. This paper summarizes the main assumptions and theoretical results of these methods to verify the solutions by detailed simulations and to demonstrate the applicability through examples relevant to the Troll and Helder fields.

Semianalytical Solution

Physical Model Description. Fig. 1 is a sketch of the vertical cross section. The horizontal well is located at the origin of the Cartesian coordinate system (x,y), with the original gas/oil contact (GOC) at D_g and the original water/oil contact (WOC) at D_w. The coordinates (x_g,y_g) and (x_w,y_w) denote points on the moving boundaries between gas and oil and water and oil, respectively. Initially, the two interfaces are horizontal planes. After production begins, their time-dependent deflection toward the well, indicated in Fig. 1, is calculated from the semianalytical solution.

Gravity equilibrium is assumed in both gas and water phases. This assumption is valid at low rates and implies that only the diffusivity equation for oil has to be solved. Water- and gas-phase mobilities therefore do not take part in the semianalytical solution, but their densities are incorporated through the moving-boundary conditions. (Another solution, based on the assumption of constant pressure at the moving boundary is briefly discussed under Single-Cone Solution.)

The well is a horizontal, infinitely long line sink, and the reservoir has no fixed boundaries. The solution is therefore valid in the infinite-acting period, and because there is no pressure support, no critical rate is expected. The flux is uniform and constant along the well axis, and the reservoir is homogeneous and anisotropic. Other assumptions are incompressible fluids, zero capillary pressure, sharp fluid interfaces, and complete displacement with no residual oil left by either displacing phase.

Mathematical Formulation, Two-Cone Problem. The fluid-flow equation for incompressible oil is

$$\frac{k_H}{k_V}\frac{\partial^2\Phi}{\partial x^2}+\frac{\partial^2\Phi}{\partial y^2}=\frac{1}{1.1271\times10^{-3}}\frac{\mu_o q_o B_o}{k_V L}\delta(x)\delta(y), \quad \ldots\ldots(1)$$

where δ is the Dirac delta function. The flow potential is defined by

$$\Phi(x,y,t)=p_o(x,y,t)+(\rho_o y/144)-p_o(\infty,0,0). \quad \ldots\ldots\ldots\ldots(2)$$

The quasistatic boundary conditions are explained with reference to the two points with coordinates (x_w,y_w) and (x_g,y_g) in Fig. 1. On the oil/water interface, we have the following relations:

$$p_w(x_w,-D_w)=p_w(x_w,y_w)-(\rho_w/144)(D_w+y_w),$$

$$p_w(x_w,y_w)=p_o(x_w,y_w),$$

and $$p_w(x_w,-D_w)=p_w(\infty,-D_w)=p_o(\infty,-D_w)$$
$$=p_o(\infty,0)+\rho_o D_w/144.$$

Combining these equations and using Eq. 2, we obtain

$$\Phi(x_w,y_w)=-[(\rho_w-\rho_o)/144](y_w+D_w), \quad \ldots\ldots\ldots\ldots(3)$$

and, in the same manner, for a point on the gas/oil interface,

$$\Phi(x_g,y_g)=[(\rho_o-\rho_g)/144](y_g-D_g). \quad \ldots\ldots\ldots\ldots(4)$$

For simplicity, the time dependence has not been explicitly stated in all the equations. In Eqs. 3 and 4 especially, keep in mind that Φ, y_w, and y_g are time-dependent.

The dimensionless coordinates x_D and y_D are defined by

$$x_D=\sqrt{(k_V/k_H)}\,(x/h) \quad \ldots\ldots\ldots\ldots(5a)$$

and $$y_D=y/h. \quad \ldots\ldots\ldots\ldots(5b)$$

(Note that we use the formation height, h, as the normalizing length scale instead of D_g, which is used in Ref. 7. If D_g is used, the dimensionless rate and time are dependent on well placement.) Eq. 1 may then be written as

$$\frac{\partial^2\Phi}{\partial x_D^2}+\frac{\partial^2\Phi}{\partial y_D^2}=\frac{1}{1.1271\times10^{-3}}\frac{\mu_o q_o B_o}{L\sqrt{k_V k_H}}\delta(x_D)\delta(y_D). \quad \ldots\ldots(6)$$

Eq. 2 becomes

$$\Phi(x_D,y_D,t)=p_o(x_D,y_D,t)+(\rho_o h/144)y_D-p_o(\infty,0,0), \quad \ldots\ldots(7)$$

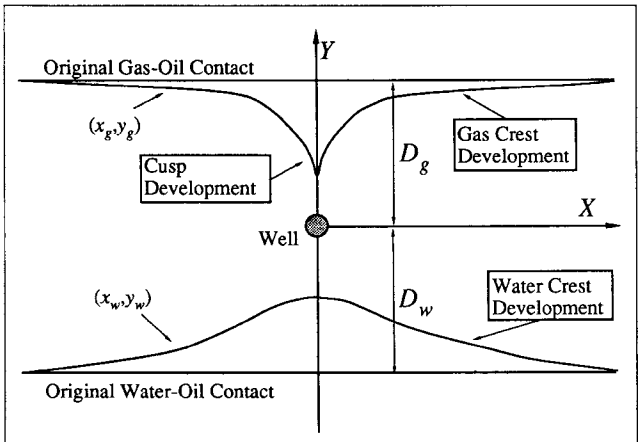

Fig. 1—Schematic vertical cross section through horizontal well and reservoir. Development of gas and water cones indicated.

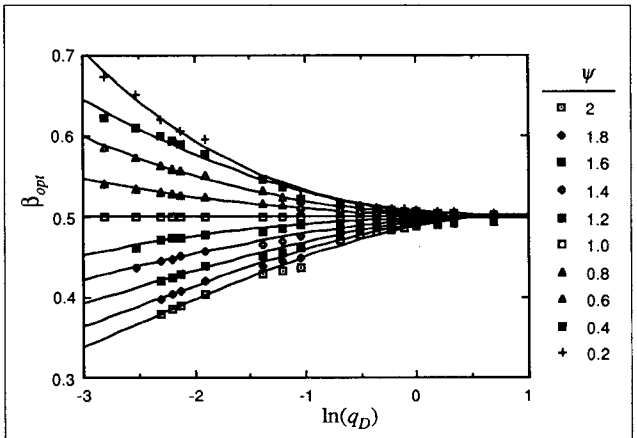

Fig. 2—Optimum well placement as a function of dimensionless rate, two-cone case.

and Eq. 3 is transformed into

$$\Phi(x_{wD},y_{wD},t)=-\frac{h(\rho_w-\rho_o)}{144}[y_{wD}(t)+\beta], \quad \ldots\ldots\ldots\ldots (8)$$

with the fractional well placement defined by

$$\beta=D_w/h \quad \ldots\ldots\ldots\ldots (9)$$

and the oil zone height by $h=D_g+D_w$. Eq. 4 becomes

$$\Phi(x_{gD},y_{gD},t)=\frac{h(\rho_o-\rho_g)}{144}[y_{gD}(t)-1+\beta]. \quad \ldots\ldots\ldots\ldots (10)$$

Dimensionless potential and rate are defined by

$$\Phi_D=144\Phi/h(\rho_o-\rho_g) \quad \ldots\ldots\ldots\ldots (11)$$

and $$q_D=\frac{144}{1.1271\times10^{-3}}\frac{\mu_o q_o B_o}{2\pi L\sqrt{k_V k_H}\,h(\rho_o-\rho_g)}, \quad \ldots\ldots\ldots\ldots (12)$$

and Eqs. 6 through 8 become, respectively,

$$\frac{\partial^2\Phi_D}{\partial x_D^2}+\frac{\partial^2\Phi_D}{\partial y_D^2}=2\pi q_D\delta(x_D)\delta(y_D), \quad \ldots\ldots\ldots\ldots (13)$$

$$\Phi_D(x_D,y_D,t)=\frac{p(x_D,y_D,t)+(hy_D\rho_o/144)-p(\infty,0,0)}{h(\rho_o-\rho_g)/144}, \quad \ldots (14)$$

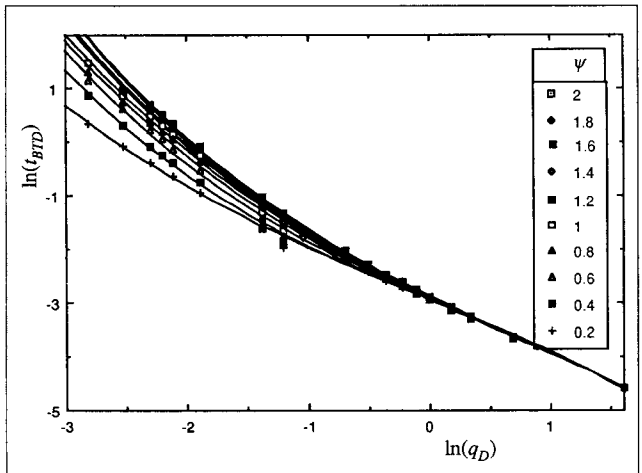

Fig. 3—Dimensionless time for simultaneous breakthrough as a function of dimensionless rate, two-cone case.

and $$\Phi_D(x_{wD},y_{wD},t)=-\psi[y_{wD}(t)+\beta], \quad \ldots\ldots\ldots\ldots (15)$$

where the density contrast is given by

$$\psi=(\rho_w-\rho_o)/(\rho_o-\rho_g) \quad \ldots\ldots\ldots\ldots (16)$$

and Eq. 10 is replaced by

$$\Phi_D(x_{gD},y_{gD},t)=y_{gD}(t)-1+\beta. \quad \ldots\ldots\ldots\ldots (17)$$

The dynamic boundary conditions are found by applying Darcy's law to the upper and lower interfaces:

$$\frac{\partial x_B}{\partial t}=-6.3283\times10^{-3}\frac{k_H}{\phi\mu_o}\frac{\partial\Phi}{\partial x_B} \quad \ldots\ldots\ldots\ldots (18a)$$

and $$\frac{\partial y_B}{\partial t}=-6.3283\times10^{-3}\frac{k_V}{\phi\mu_o}\frac{\partial\Phi}{\partial y_B}, \quad \ldots\ldots\ldots\ldots (18b)$$

where index $B=g$ for the upper boundary and w for the lower boundary (Fig. 1). With the dimensionless quantities x_D, y_D, and Φ_D already introduced and

$$t_D=\frac{6.3283\times10^{-3}}{144}\frac{(\rho_o-\rho_g)k_V}{h\phi\mu_o}t, \quad \ldots\ldots\ldots\ldots (19)$$

Eqs. 18 can be written

$$\frac{\partial x_{BD}}{\partial t_D}=-\frac{\partial\Phi_D}{\partial x_{BD}} \quad \ldots\ldots\ldots\ldots (20a)$$

and $$\frac{\partial y_{BD}}{\partial t_D}=-\frac{\partial\Phi_D}{\partial y_{BD}}. \quad \ldots\ldots\ldots\ldots (20b)$$

Eqs. 13, 15, 17, and 20 constitute the flow equation with boundary conditions, and the initial condition is gravity equilibrium. For

TABLE 1—COEFFICIENTS IN THIRD-ORDER POLYNOMIAL FOR OPTIMUM WELL PLACEMENT

ψ	C_0	C_1	C_2	C_3
0.2	0.507	−0.0126	0.01055	−0.002483
0.4	0.504	−0.0159	0.01015	−0.000096
0.6	0.503	−0.0095	0.00624	−0.000424
0.8	0.502	−0.0048	0.00292	−0.000148
1.0	0.500	−0.0001	0.00004	0.000009
1.2	0.497	0.0042	−0.00260	0.000384
1.4	0.495	0.0116	−0.00557	−0.000405
1.6	0.493	0.0178	−0.00811	−0.000921
1.8	0.490	0.0231	−0.01020	−0.001242
2.0	0.488	0.0277	−0.01189	−0.001467

TABLE 2—COEFFICIENTS IN THIRD-ORDER POLYNOMIAL FOR BREAKTHROUGH TIME, t_{BTD}, TWO-CONE CASE

ψ	C_0	C_1	C_2	C_3
0.2	−2.9494	−0.94654	−0.0028369	−0.029879
0.4	−2.9473	−0.93007	0.016244	−0.049687
0.6	−2.9484	−0.9805	0.050875	−0.046258
0.8	−2.9447	−1.0332	0.075238	−0.038897
1	−2.9351	−1.0678	0.088277	−0.034931
1.2	−2.9218	−1.0718	0.091371	−0.040743
1.4	−2.9162	−1.0716	0.093986	−0.042933
1.6	−2.9017	−1.0731	0.094943	−0.048212
1.8	−2.8917	−1.0856	0.096654	−0.046621
2	−2.8826	−1.1103	0.10094	−0.040963

a constant production rate, the solution contains the well placement, β, and the density contrast, ψ, as parameters and is given in principle by Papatzacos and Gustafson,[7] although with slightly different dimensionless variables.

Results. A FORTRAN program is used to calculate the development of the two interfaces. For a given q_D and ψ, the program searches for the optimum well placement, β_{opt}, through a series of cone-development runs. This optimum well placement, with the longest breakthrough time, is found by shifting the well position along the y axis until both phases cusp into the well simultaneously. Numerical errors are introduced by the timestep procedure, the convergence acceleration, and roundoff. The total error is estimated at 5 to 10%.

Fig. 2 gives β_{opt} as a function of dimensionless rate with the density contrast as a parameter, and **Fig. 3** gives the corresponding dimensionless breakthrough time. The two numerical methods used for high and low rates do not overlap around $q_D=0.4$, but the gap is small and negligible.

To facilitate practical use of the results, each series of points, for a given ψ, has been curve fitted with a third-order polynomial. **Tables 1 and 2** list the coefficients. The polynomial has the form

$$V=C_0+C_1U+C_2U^2+C_3U^3, \quad \ldots\ldots\ldots\ldots\ldots\ldots (21)$$

where $V=\beta_{opt}$ for Table 1 coefficients and $\ln(t_{BTD})$ for Table 2 coefficients and $U=\ln(q_D)$ in both cases. Note that the lowest data point in the two figures is for $q_D=0.06$ and that extrapolation below this value is not recommended.

The optimum well placement and the corresponding breakthrough time become independent of ψ for $q_D>1$, as Figs. 2 and 3 show. The well is then placed in the middle of the oil zone, as could have been expected.

In practical use, q_D is first calculated from Eq. 12 and ψ from Eq. 16. Then, t_{BTD} and β_{opt} are found from the graphs or the polynomials.

Well at an Impervious Oil-Zone Top or Bottom. $\psi=1.0$ defines a horizontal symmetry plane through the well in the middle of the oil zone, with $\beta_{opt}=0.5$ for all rates, from Fig. 2. Therefore, using the two-cone solution with $\psi=1.0$, twice the rate, twice the oil-zone height, and the other actual reservoir parameters is equivalent to placing the well at an impervious top or bottom of the oil zone. The density difference to be used in Eqs. 12 and 19 is $(\rho_o-\rho_g)$ for a single gas cone and $(\rho_w-\rho_o)$ for a single water cone.

Single-Cone Solution. A similar derivation has been carried out for the single-cone problem[8,9] when only one fluid contact is present. For the single-cone water case, the density difference between water and oil, $(\rho_w-\rho_o)$, has to be used instead of $(\rho_o-\rho_g)$ in Eqs. 12 and 19. The single-cone gas case corresponds to having the water phase in Fig. 1 substituted by oil. The well is now placed at a fixed distance D_g below the initial GOC and the time to breakthrough is a function of the production rate only. The dimensionless variables are defined as in the two-cone case, with the sole exception

TABLE 3—COEFFICIENTS IN THIRD-ORDER POLYNOMIAL FOR BREAKTHROUGH TIME, SINGLE-CONE CASE, $q_D<0.4$

C_0	C_1	C_2	C_3
−1.7179	−1.1633	0.16308	−0.046508

that D_g rather than h is the normalizing length scale in all expressions (e.g., Eqs. 12 and 19).

In Ref. 10, a different approach is taken for the single-cone problem. Instead of gravity equilibrium in the cone, constant pressure is assumed on the moving boundary. The solution is found by complex analysis and conformal mapping, with the time to breakthrough given by

$$t_{BTD}=1/6q_D. \quad \ldots\ldots\ldots\ldots\ldots\ldots\ldots\ldots\ldots\ldots (22)$$

The details of the solution of the present model, with gravity equilibrium in the cone, can be found in Refs. 8 and 9. As in the two-cone case, the procedure is different for high and low rates. When $q_D<0.4$, the fast Fourier transform with convergence acceleration (FFT-CA) is used. For $q_D>0.4$, it is possible to close the iteration procedure[8] and explicitly determine

$$t_{BTD}=1-(3q_D-1)\ln[3q_D/(3q_D-1)]. \quad \ldots\ldots\ldots\ldots\ldots (23)$$

By series expansion, Eq. 23 becomes equal to Eq. 22 when q_D is large; i.e., the assumption of vertical equilibrium in the cone is then equivalent to a moving constant-pressure boundary.

Fig. 4 shows results when the FFT-CA procedure is used together with the results from Eq. 22 and Eq. 23. There is virtually no difference between Eqs. 22 and 23 when $q_D>1$. Eq. 23 slightly bypasses the FFT-CA results in an interval around $q_D=0.4$ without direct overlap. For $q_D=0.4$, Eq. 23 gives $t_{BTD}=0.64$, compared with 0.62 for the FFT-CA procedure. A third-order polynomial was fitted to all the data points from the FFT-CA procedure and Eq. 23 combined. The polynomial is intended for values $q_D<0.4$, while Eq. 23 may be used directly for larger values. The polynomial is of the same form as in Eq. 21, with $V=\ln(t_{BTD})$ and the coefficients given in **Table 3**. The last data point is for $q_D=0.1$; extrapolation below this value is not recommended.

Eq. 23 cannot be used below $q_D=⅓$, but gives the limiting value $t_{BTD}=1$ when $q_D\to⅓$, which is very close to the FFT-CA value, as can be seen from Fig. 4. Eq. 23 can therefore be applied with good accuracy for $q_D>⅓$.

Numerical Simulation

Three different cases have been studied, the two-cone case with simultaneous gas and water coning, the single-cone gas case, and the single-cone water case.[11,12] Most of the work has been concentrated on the first two cases; particularly the gas-cone case has been tested extensively for numerical dispersion effects.

Model. The aim of the numerical simulation study is to quantify the accuracy of the semianalytical solution. We therefore used a standard commercial black-oil model without any modifying assumptions.

Grid and Dispersion. The simulation runs are limited to the vertical cross section in Fig. 1. A slab in the z direction was used, with the cross section represented by the xy plane and the horizontal well along the z axis. We used a regular Cartesian grid without any local refinement. **Fig. 5** is a schematic of the grid. Because of symmetry, simulation of half the cross section is sufficient.

Many simulation runs were made to select a grid that would give results unhampered by numerical dispersion. As expected, the vertical dimension required more blocks than the horizontal. Many layers were also needed in the gas and water zones to make the system behave in an infinite-acting manner, and fine-gridding had to be applied across the original fluid contacts. Simulating the gas zone by a thin layer with large PV, for instance, is essentially equivalent to a constant-pressure boundary and a cone development more in line with Eq. 22 than Eq. 23. After some trials, we ended with

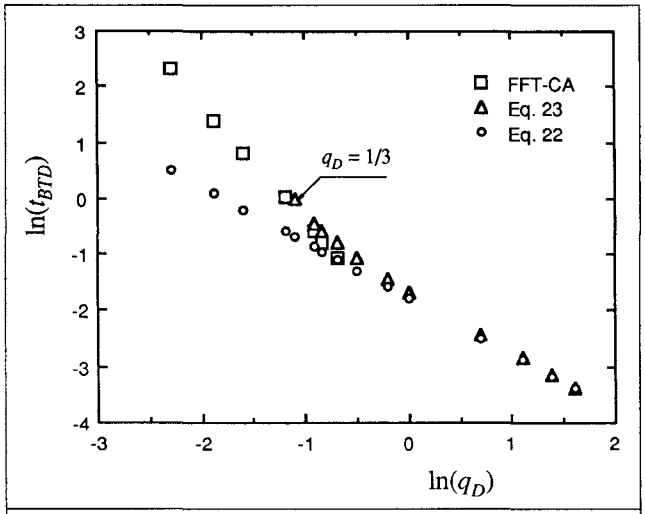

Fig. 4—Semianalytical solutions for the single-cone case.

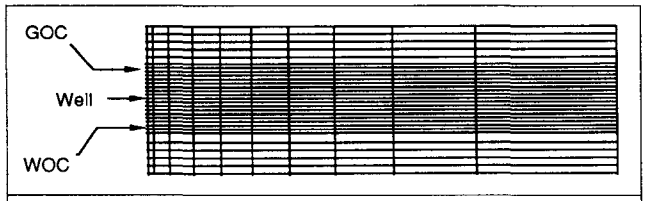

Fig. 5—Schematic of numerical grid.

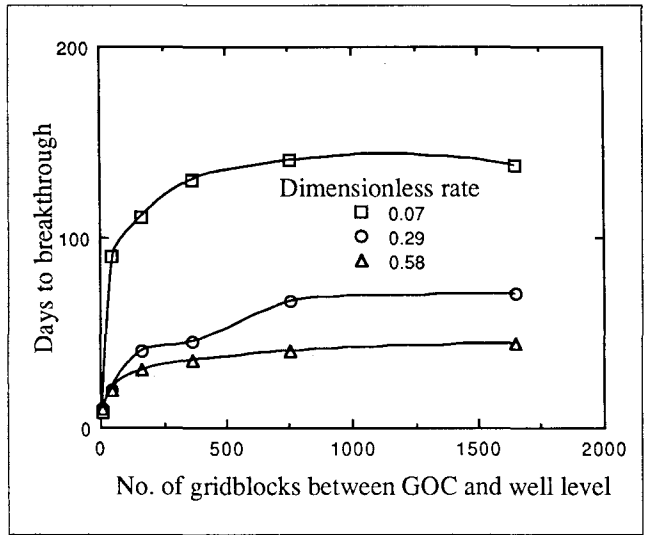

Fig. 6—Breakthrough time as a function of number of gridblocks between GOC and the well, single-cone gas case.

a uniform vertical grid within the oil zone, coarsening into the gas and water zones, and a horizontal grid with spacing increasing from the well. The rationale for the uniform gridding in the oil zone is to have a good definition of the interface movement, and because the breakthrough essentially occurs when a cusp forms at a distance from the well,[7] graded gridding close to the well was considered unnecessary, although it may have some influence at high rates.

Fig. 6 shows how the required number of gridblocks was determined in the cross section between the well level and the initial GOC for the single-cone case. The number of gridblocks is for the total cross section. More than 1,000 blocks are required. As listed in **Table 4**, $40 \times 18 = 720$ blocks for the half plane, or 1,440 for the total cross section, were finally chosen. Up to 5,500 blocks in

TABLE 4—GAS-CONE CASE

Grid	
Number of gridblocks	$18 \times 80 \times 1 = 1{,}440$
x-direction block sizes, ft	1, 2, 4, 6, 8, 10, 15, 20, 30, 50, 75, 100, 250, 500, 1,000, 1,500, 2,500, 5,000
y-direction block sizes, ft from top	1,000, 750, 500, 250, 100, 50, 5×10, 5×3, 3×2.5, (GOC), 40×1.14, 1 (well), 10×2.5, 5×5, 5×10
z-direction block size, ft	80

Reservoir Parameters*	
General	
p_i at GOC, psia	2,290
k_H, md	1,000 to 5,580
k_V, md	100 to 1,000
D_g, ft	45.6
ϕ	0.31
Fluids	
ρ_o (res. cond.), lbm/ft^3	42.23
ρ_g (res. cond.), lbm/ft^3	10.00
B_o, RB/STB	1.16
μ_o, cp	1.6
μ_g, cp	0.005 to 0.15

Relative Permeabilities

S_g	k_{rg}	S_o	k_{ro}
0.10	0.00	0.10	0.00
0.15	0.04	0.25	0.007
0.20	0.07	0.30	0.07
0.25	0.10	0.70	0.70
0.30	0.14	1.00	1.00
0.35	0.19		
0.40	0.23		
0.45	0.30		
0.50	0.38		
0.60	0.53		
0.65	0.67		
1.00	1.00		

*Other parameters were the same as in Ref. 13.

TABLE 5—TWO-CONE CASE

Grid	
Number of gridblocks	$15 \times 155 \times 1 = 2{,}325$
x-direction block sizes, ft	0.5, 1, 2, 4, 8, 16, 32, 64, 128, 256, 512, 1,024, 2,048, 4,096, 5,000
y-direction block sizes, ft from top	20×164.65, 80, 56.5, 36.5, 12, 6, 4, 2, 10×1, (GOC), 48×0.8229, 1 (well), 32×1.2344, (WOC), 10×1, 2, 4, 6, 12, 20, 40, 80, 20×164.65
z-direction block size, ft	1,500

Reservoir Parameters*	
General	
p_i at WOC, psia	2,290
k_H, md	5,580
k_V, md	1.8
h, ft	80
ϕ	0.31
Fluids	
ρ_o (res. cond.), lbm/ft^3	51.67
ρ_g (res. cond.), lbm/ft^3	6.99
ρ_w (res. cond.), lbm/ft^3	65.41
B_o, RB/STB	1.18
μ_o, cp	1.6
μ_g, cp	0.03
μ_w, cp	0.5

*Other parameters, relative permeabilities, and capillary pressure were the same as in Ref. 13.

TABLE 6—WATER-CONE CASE

Grid	
Number of gridblocks	$15 \times 51 \times 1 = 765$
x-direction block sizes	Same as for two-cone case
y-direction block sizes, ft from top	1,350, 750, 350, 70, 35, 4×3.718, 1 (well), 25×1.218 (WOC), 7×1.218, 1.5, 2, 6, 10, 50, 250, 500, 1,500, 2,500
z-direction block size, ft	80

Reservoir Parameters*	
General	
p_i at WOC, psia	2,290
k_H, md	5,000
k_V, md	20
D_w, ft	30.45
ϕ	0.31
Fluids	
ρ_o (res. cond.), lbm/ft^3	40.89
ρ_w (res. cond.), lbm/ft^3	64.06
B_o, RB/STB	1.10
μ_o, cp	1.6
μ_w, cp	0.15 to 1.5

Relative Permeabilities

S_g	k_{rg}	S_o	k_{ro}
0.10	0.00	0.25	0.00
0.30	0.047	0.40	0.22
0.75	0.151	0.55	0.46
0.85	0.374	0.70	0.692
1.00	1.00	0.80	0.82
		0.90	1.00

*Other parameters were the same as in Ref. 13.

the area between the well and the initial GOC were used without any noticeable change from the 1,600-block case in Fig. 6.

The breakthrough times were easily identified from plots of WOR and/or GOR vs. time and recorded when the ratios started to increase, not at the time of steepest increase. The reported times to breakthrough are therefore expected to be early because it is difficult to eliminate numerical dispersion completely.

Input Data. Tables 4 through 6 summarize typical input data sets for the three cases. Note that the vertical column of blocks farthest from the well was given a large PV to emulate an infinite reservoir in the horizontal direction. Most of the data correspond to the Troll field example.[13]

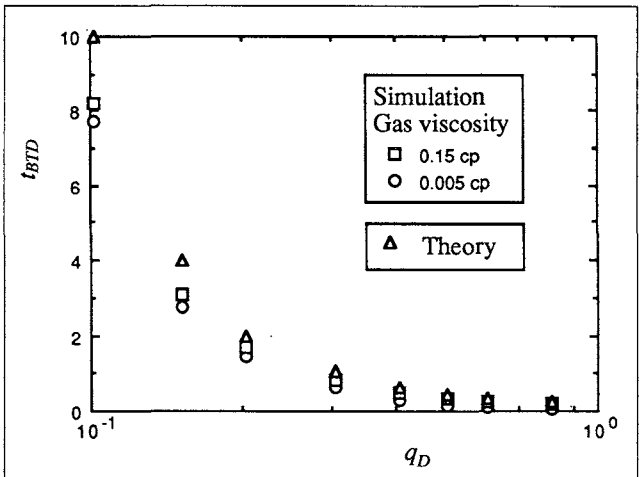

Fig. 7—Dimensionless time to breakthrough vs. dimensionless rate from theory and simulations, single-cone case.

Gas-Cone Results. About 80 simulation runs were made for different anisotropy ratios, k_V/k_H, and gas viscosities ranging from 0.005 to 0.16 cp. These extreme viscosities are rather unrealistic, but they have been included to bracket the range of natural viscosity variations. The simulated breakthrough time varied from 30 to 7,000 days for dimensionless rates between 0.1 and 0.8.

As expected, varying the anisotropy ratio for different rates gave nearly identical results when plotted on a dimensionless t_{BTD}-vs.-q_D graph for a fixed gas viscosity. The dimensionless quantities therefore correctly incorporate anisotropy. The same conclusion is also valid for the two-cone case.

Fig. 7 shows the time to breakthrough as a function of rate for high and low gas viscosity compared with the theory. The simulator breakthrough time is less, but follows the same general trend as the theory. **Fig. 8** shows the percentage error $[(t_{BTD}^{th} - t_{BTD}^{sim})/t_{BTD}^{sim}]100\%$ vs. rate for different gas viscosities. The curves converge to a relatively low error for low rates because the assumption of vertical equilibrium in the gas cone improves with decreasing rate. At the lowest rate, the error is virtually independent of the gas viscosity, consistent with the theory. The remaining error at the lowest rate can probably be explained by the amount of oil left behind the displacing gas. According to microscopic displacement theory with gravity included,[14] only immobile oil will be left in the gas cone at low rates. For the specific case discussed here, the residual oil saturation is about 0.25 (cf. Table 4). Adjusting the porosity in Eq. 19 accordingly nearly eliminates the error.

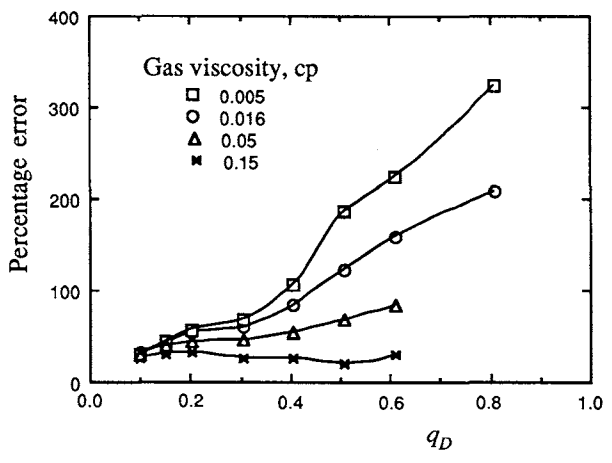

Fig. 8—Percentage error, single-cone gas case.

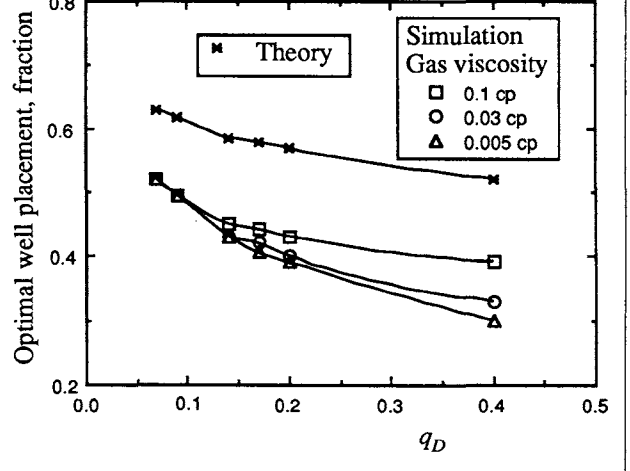

Fig. 9—Optimal well placement in fraction of oil-zone height for simultaneous breakthrough of gas and water cones.

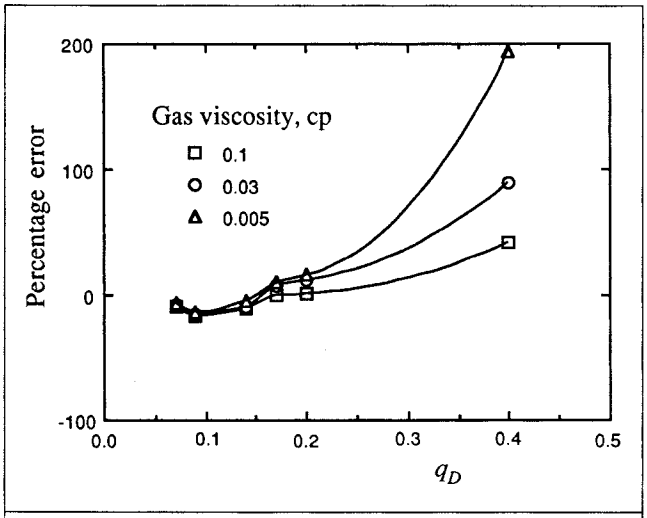

Fig. 10—Percentage error, two-cone case.

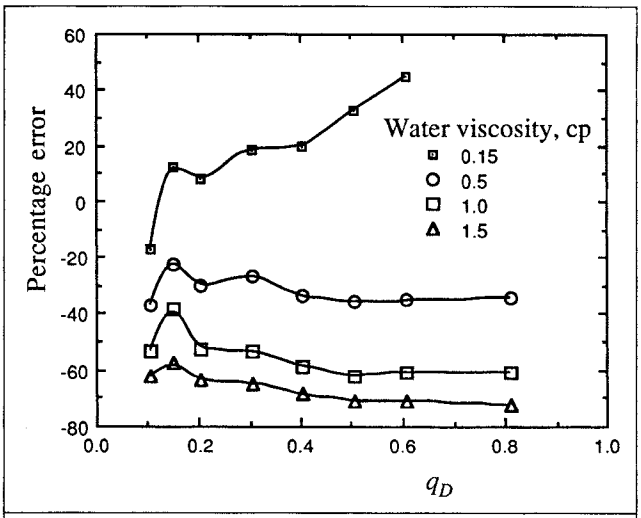

Fig. 11—Percentage error, single-cone water case.

One would perhaps have expected, contrary to the results in Fig. 8, that the error would be negative because the theory assumes the gas to be immediately available without any flow. Also, one would perhaps expect the absolute value of the error to decrease when the gas viscosity decreases because vertical equilibrium in the gas cone then is approached gradually. There are, however, at least two interacting physical effects in the simulated cone-evolution problem that could possibly explain the observed simulation results.

First, the microscopic displacement efficiency is a function of both rate and gas viscosity.[14] When the gas viscosity is reduced, more oil is left behind, making the gas cone expand faster than for a complete piston-like displacement. To demonstrate the effect, we simulated until gas breakthrough with $\mu_g=0.001$ and 0.15 cp for rates $q_D=0.30$ and 0.60. At the low rate, both viscosities gave the same average gas saturation of 0.65 in the cone. The high rate, however, gave 0.44 and 0.24 for $\mu_g=0.15$ and 0.001 cp, respectively.

Second, the dynamics of the cone evolution can be expected to change when movable oil is left in the cone. This effect is discussed by Saffman and Taylor[15] for viscous finger development. Translated to our case, the oil and gas densities and the oil viscosity can be modified such that the interface movement is the same as for piston-like displacement. The modification depends on the gas viscosity and the gas fraction left behind the advancing front. The group of terms $\mu_o/(\rho_o-\rho_g)$ in Eq. 12, after modification, will approach infinity as the gas fraction goes to zero, with a steep increase for a gas fraction (in terms of movable PV) <0.2, for our data set. Below this value, the properly adjusted dimensionless rate will increase and the corresponding breakthrough time from theory will decrease, thus compensating for the observed increase in percentage error.

Two-Cone Results. To determine the optimum well placement and the corresponding breakthrough time, the well was moved vertically in the oil column until the water and gas breakthrough times differed by $<2\%$.

TABLE 7—BASE-CASE PARAMETERS FOR TROLL FIELD EXAMPLE

q_o, STB/D	8,000.00
μ_o, cp	1.60
μ_g, cp	0.017
L, ft	1,500.00
k_H, md	5,580.00
k_V, md	1.80
h or D_g, ft	43.00
ρ_o, lbm/ft^3	48.67
ρ_g, lbm/ft^3	8.11
ϕ	0.31
B_o, RB/STB	1.18

Sensitivity runs were made by varying gas viscosity and holding other parameters constant at the values recorded in Table 5. **Fig. 9** compares the results with the theoretical predictions. When the rate goes to zero, gravity equilibrium is approached in the cones. The results for the three different gas viscosities converge to a single curve that has a trend toward the theoretical curve.

The optimum well placement should have been above the middle of the oil column because gas gravity is less than water gravity. For high simulation rates, however, we see from Fig. 9 that the optimum placement gradually decreases below the middle as the rate increases. Departure from gravity equilibrium will occur first in the water phase, which has the highest viscosity. To compensate, the well has to be placed closer to the initial WOC to have simultaneous breakthrough. Hence, for the highest gas viscosity, closest to that of water, the simulation results are closest to the theory.

Fig. 10 plots the percentage error. The error approaches zero when the rate decreases. For high rates, the error increases as the viscosity is reduced. These trends are the same as in the single-cone case.

In Fig. 10, the error is 90% for $q_D=0.4$ with $\mu_g=0.03$. Whether this error level is acceptable depends on the actual case.

TABLE 8—BREAKTHROUGH TIME FOR GAS CONE AND GAS/WATER CONES FOR BASE-CASE PARAMETERS

Parameter	q_D	t_{BTD} From Theory		t_{BT}, years	
		Gas/Water*	Gas**	Gas/Water*	Gas**
q†					
16,000	2.34	0.02	0.07	0.43	1.36
8,000	1.17	0.05	0.16	0.83	2.89
4,000	0.58	0.09	0.36	1.59	6.62
k_V					
100	0.16	0.43	3.65	0.14	1.19
10	0.50	0.10	0.46	0.34	1.49
1	1.57	0.03	0.11	1.13	3.76
k_H					
10,000	0.87	0.06	0.22	1.08	4.03
5,000	1.23	0.04	0.15	0.79	2.71
1,000	2.76	0.02	0.06	0.36	1.15
h or D_g‡					
30	1.67	0.03	0.11	0.41	1.36
40	1.26	0.04	0.15	0.72	2.48
50	1.00	0.05	0.19	1.11	3.98

*Two-cone gas/water case, optimum well placement in the oil column.
**Single-cone gas case, well placed at original WOC.
†Total rate for the single-cone gas case, oil rate for the gas/water case.
‡For the single-cone gas case, $D_g=h$, well at original WOC.

TABLE 9—BREAKTHROUGH TIME FOR GAS CONE AND GAS/WATER CONES, CHANGES FROM BASE CASE: 90-ft OIL COLUMN, 4,000 STB/D

Parameter	q_D	t_{BTD} From Theory		t_{BT}, years	
		Gas/Water*	Gas**	Gas/Water*	Gas**
$q^{\dagger}$					
8,000	0.56	0.09	0.38	3.49	14.4
4,000	0.28	0.20	1.14	7.46	43.3
k_V					
10	0.12	0.67	7.09	4.57	48.6
1	0.37	0.14	0.69	9.55	47.2
k_H					
10,000	0.21	0.28	1.99	10.83	75.6
5,000	0.29	0.18	1.03	6.98	39.3
1,000	0.66	0.08	0.30	2.96	11.5
h or D_g ‡					
70	0.36	0.15	0.74	4.33	21.9
80	0.31	0.17	0.92	5.76	31.3
90	0.28	0.20	1.14	7.46	43.3

*Two-cone gas/water case, optimum well placement in the oil column.
**Single-cone gas case, well placed at original WOC.
†Total rate for the single-cone gas case, oil rate for the gas/water case.
‡For the single-cone gas case, $D_g = h$, well at original WOC.

For the data set in Table 5, the breakthrough time at this rate is 1,570 days and the error is hardly acceptable. For the same data set, but with k_V=40 md and k_H=250 md, the breakthrough time is 71 days and the error is of less practical significance.

Water-Cone Results. Fig. 11 shows the percentage error. The curves have a trend toward zero as the rate decreases. The curves will meet at lower q_D values than in Fig. 8 because high water viscosity requires lower rates to achieve the same degree of gravity equilibrium. For the three highest viscosities, which are all higher than the oil viscosity, the error is negative and decreases with increasing viscosity. The water cone is therefore far from gravity equilibrium. In fact, the water influx into the oil zone clearly depends on the water viscosity, as we have observed from the simulations. The 0.15-cp case in Fig. 11, included for comparison, shows the same features as for gas: positive error that increases with rate.

Sample Calculation

Troll Data. The example is taken from the Troll field, and **Table 7** gives the reservoir parameters for the base case, which are close to those for the base case in Ref. 13. The vertical and horizontal permeabilities are harmonic and arithmetic averages, respectively, of the individual layer permeabilities.

Sensitivity Cases. Table 8 shows the results of separately varying the rate, vertical and horizontal permeability, and oil-zone thickness. For each section of Table 8, only the indicated parameter is varied, while the others are kept at their base values. The exercise is repeated in **Table 9** with two changes in the base parameters of Table 7: the oil rate is 4,000 STB/D and the oil column thickness is 90 ft.

In the Troll field, the oil-zone thickness reportedly[13] varies between 0 and 92 ft. For the two-cone cases, the well is assumed to be placed optimally, with simultaneous breakthrough of gas and water. The data in Table 7 give ψ=0.40, and the corresponding coefficients from Table 2 were used to calculate the breakthrough time.

For the single gas cone, the well is placed at the initial WOC. If the processing equipment can handle large amounts of water, this is a viable well placement for oil recovery. The main problem is to avoid gas breakthrough, which will practically terminate the oil production.

Tables 8 and 9 demonstrate that the theory predicts results of practical interest, especially for the low dimensionless rates that have small percentage errors.

TABLE 10—HELDER FIELD PARAMETERS FOR THEORETICAL PREDICTIONS

μ_o, cp	28.90
L, ft	440.00
k_H, md	3,680.00
k_V, md	2,944.00
ρ_w, lbm/ft^3	66.77
ρ_o, lbm/ft^3	54.91
ϕ	0.30*
B_o, RB/STB	1.06

	Infinite oil column, single-cone solution	Well at top, two-cone solution
q_o, STB/D	2,000.00	4,000.00
h or D_g, ft**	71.00	142.00
t_{BT}, days	74	42

*Assumed
**D_g for single-cone, h for two-cone case.

Comparison With Helder Field Tests

Table 10 shows the reservoir parameters required to make theoretical predictions for the Helder field.[16] The parameters correspond to horizontal Well A-4, which was drilled close to the top of the oil zone. A recorded minimum value of 71 ft is used for the vertical distance between the WOC and the well.

The time to breakthrough can be estimated from the single-cone solution if the oil column height is assumed to be infinite. This estimate is improved by incorporating the actual no-flow boundary condition at the top of the oil zone. We then set ψ=1 and double both the production rate and oil-zone height indicated in Table 10. The single-cone solution (Eq. 23) gives a water breakthrough time of 74 days, and the two-cone solution, with coefficients from Table 2, gives 42 days at a dimensionless rate q_D=1.02. The measured breakthrough time is 10 days.[16]

There are, of course, many factors that may explain the difference between the best estimate of 42 days and the measured 10 days. For instance, the porosity is assumed to be 0.30 in Table 10. Using a lower effective porosity adjusted for the oil saturation in the cone will decrease the theoretical time to breakthrough. Also, the vertical permeability value is uncertain in Ref. 16 and is estimated at a factor 0.8 times the horizontal permeability.

Conclusions

1. A semianalytical theory was developed for predicting single-cone gas or water and two-cone gas and water breakthrough times in horizontal wells completed in the oil zone.
2. The two-cone solution predicts single-cone water or gas breakthrough time if the well is located at the impervious top or bottom, respectively, of the oil zone.
3. For the single-cone case, a simple expression is given for the breakthrough time for $q_D > \frac{1}{3}$.
4. The simulation studies show that the theory is valid for low dimensionless rates, when the time to breakthrough is sufficiently long to be of practical interest, and error estimates are given.
5. The theory shows that horizontal-well drainage from the thin oil zone in the Troll field is a definite possibility and predicts breakthrough times that compare favorably with field test results from the Helder field.

Nomenclature

B = FVF, RB/STB
C = coefficient in polynomial, Eq. 21
D_g = depth of well below original GOC, ft
D_w = depth below well of original WOC, ft
h = oil-zone height, ft
k = permeability, md
L = well length, ft
p = pressure, psi
q = flow rate, STB/D

Authors


Papatzacos

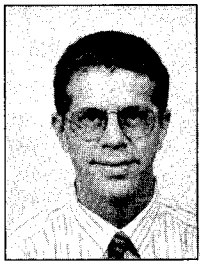
Herring

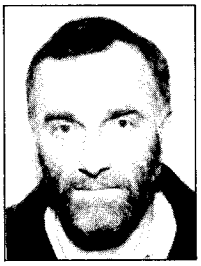
Skjaeveland


Martinesen

Paul Papatzacos is assistant professor of mathematics at Rogaland U. Centre in Stavanger and consultant to the Rogaland Research Inst. He holds a degree in engineering from the Ecole Natl. Supérieure de l'Aeronautique in Paris and a PhD degree in elementary particle physics from the U. of Trondheim. **Todd Herring** is a reservoir engineer with Fina Exploration Norway in Stavanger with interests in reservoir modeling. He holds BS and MS degrees in petroleum engineering from Rogaland U. **Rune Martinsen** is an engineer at Enterprise Oil Norway Ltd. in Stavanger. His primary interests are in numerical simulation and horizontal-well applications. He holds BS and MS degrees in petroleum engineering from Rogaland U. **Svein M. Skjaeveland** is a professor of petroleum engineering at Rogaland U. He holds PhD degrees in physics from the Norwegian Inst. of Technology in Trondheim and in petroleum engineering from Texas A&M U. Skjaeveland was 1979–87 SPE Student Chapter faculty sponsor and a Section Director during 1986–87. He was elected 1990 Oil Man of the Year by the Stavanger Section and president of Rogaland U. for 1992–94. He also is currently a member of the Editorial Review Committee.

t = time, days
U,V = variables in polynomial, Eq. 21
v = velocity of fluid interface, ft/D
x,y,z = Cartesian coordinates, ft
$\beta = D_w/h$, fractional well placement
Δ = difference operator
μ = viscosity, cp
ρ = density, lbm/ft^3
ϕ = porosity
Φ = flow potential, psi
ψ = density contrast, Eq. 16

Subscripts
B = boundary
BT = breakthrough
D = dimensionless
g = gas
H = horizontal
o = oil
opt = optimum
V = vertical
w = water

Superscripts
sim = from simulation
th = from theory

Acknowledgment

We are grateful to the Norwegian Research Council for Science and the Humanities for computing time.

References

1. Ekrann, S.E.: "Production From Thin Oil Zones," technical report No. SPT T-6/87, Rogaland Research Inst., Stavanger (Sept. 29, 1987).
2. Joshi, S.D.: "A Review of Horizontal Well and Drainhole Technology," paper SPE 16868 presented at the 1987 SPE Annual Technical Conference and Exhibition, Dallas, Sept. 27–30.
3. Giger, F.M.: "Analytic Two-Dimensional Models of Water Cresting Before Breakthrough for Horizontal Wells," *SPERE* (Nov. 1989) 409–16; *Trans.*, AIME, **287**.
4. Karcher, B.J., Giger, F.M., and Combe, J.: "Some Practical Formulas To Predict Horizontal Well Behavior," paper SPE 15430 presented at the 1986 SPE Annual Technical Conference and Exhibition, New Orleans, Oct. 5–8.
5. Chaperon, I.: "Theoretical Study of Coning Toward Horizontal and Vertical Wells in Anisotropic Formations: Subcritical and Critical Rates," paper SPE 15377 presented at the 1986 SPE Annual Technical Conference and Exhibition, New Orleans, Oct. 5–8.
6. Muskat, M. and Wyckoff, R.D.: "Approximate Theory of Water-Coning in Oil Production," *Trans.*, AIME (1935) **114**, 144–61.
7. Papatzacos, P. and Gustafson, S.-Å.: "Incompressible Flow in Porous Media With Two Moving Boundaries," *J. Comp. Phys.* (1988) **78**, 231–48.
8. Papatzacos, P.: "Gas Coning by a Horizontal Well," *Well-Test Analysis*, Rogaland Research Inst., Stavanger (March 1989) Report K-63/89.
9. Papatzacos, P.: "Gas Coning by a Horizontal Well as a Moving Boundary Problem," *Proc.*, European Conference on Mathematics of Oil Recovery, Cambridge (July 25–27, 1989).
10. Larsen, L. and Papatzacos, P.: "Well-Test Analysis of Pressure-Transient Data Influenced by Coning Effects," *Well-Test Analysis*, Rogaland Research Inst., Stavanger (Aug. 1987) Report K-44/87.
11. Herring, T.R.: "Simultaneous Gas and Water Coning in Horizontal Wells—A Simulation Study," MS thesis, Rogaland U., Stavanger (1989).
12. Martinsen, R.: "Gas Cresting Toward a Horizontal Well—A Simulation Study," MS thesis, Rogaland U., Stavanger (1989).
13. Kossack, C.A., Kleppe, J., and Aasen, T.: "Oil Production From the Troll Field: A Comparison of Horizontal and Vertical Wells," paper SPE 16869 presented at the 1987 SPE Annual Technical Conference and Exhibition, Dallas, Sept. 27–30.
14. Buckley, S.E. and Leverett, M.C.: "Mechanisms of Fluid Displacement in Sands," *Trans.*, AIME (1942) **146**, 107–16.
15. Saffman, P.G. and Taylor, G.I.: "The Penetration of a Fluid into a Porous Medium or Hele-Shaw Cell Containing a More Viscous Fluid," *Proc.*, Royal Soc., London (1958) **A245**, 312–29.
16. Murphy, P.J.: "Performance of Horizontal Wells in the Helder Field," *JPT* (June 1990) 792–800; *Trans.*, AIME, **289**.

SI Metric Conversion Factors

bbl	× 1.589 873	E−01	= m^3
cp	× 1.0*	E−03	= Pa·s
ft	× 3.048*	E−01	= m
lbm/ft^3	× 1.601 846	E+01	= kg/m^3
md	× 9.869 233	E−04	= μm^2

*Conversion factor is exact.

SPERE

Original SPE manuscript received for review Oct. 9, 1989. Paper accepted for publication Sept. 18, 1990. Revised manuscript received Aug. 28, 1990. Paper (SPE 19822) first presented at the 1989 SPE Annual Technical Conference and Exhibition held in San Antonio, Oct. 8–11.